# STRUCTURAL CHARACTERIZATION AND GAS REACTIONS OF SMALL METAL PARTICLES BY HIGH RESOLUTION IN-SITU TEM AND TED

Periodic Technical Report

for
Cooperative Agreement NCC2-283

for the period
January 1, 1986 - December 31, 1986

Submitted to

National Aeronautics and Space Administration
Ames Research Center
Moffett Field, California 94305

Computational Chemistry Branch
Dr. David Cooper, Chief and Technical Monitor

Thermosciences Division
Dr. Jim Arnold, Chief

Prepared by

ELORET INSTITUTE
1178 Maraschino Drive
Sunnyvale, CA 94087
(phone: 408 730-8422)
Klaus Heinemann, President and Principal Investigator
2 January, 1987

# STRUCTURAL CHARACTERIZATION AND GAS REACTIONS OF SMALL METAL PARTICLES BY HIGH RESOLUTION IN-SITU TEM AND TED

The detection and size analysis of small metal particles supported on amorphous substrates becomes increasingly difficult when the particle size approaches that of the phase contrast background structures of the support. In addition, size determinations of such small particles are significantly affected by the TEM imaging conditions, such as focus and astigmatism correction. Palladium particles of less than 2 nm mean size were examined by high resolution TEM and subsequent electronic image analysis, using a Quantimet 720 Image Analyzer. A deviation of only a few hundred nm from the optimum focus condition was, for example, found to increase the "apparent" diameter of 1.3 nm particles by as much as 0.4 nm. Furthermore, the electron exposure required to perform very high resolution microscopy may severely complexify the situation by radiation induced changes in specimen and support. These changes may be intensified by specimen contaminants and improperly controlled environment. An approach of digital image analysis, involving Fourier transformation of the original image, filtering, and image reconstruction was studied with respect to the likelihood of unambiguously detecting particles of less than 1 nm diameter on amorphous substrates from a single electron micrograph. A paper describing this work is in print in Ultramicroscopy (Appendix 1).

The moving and installation activities of the in-situ TEM facility to the Department of Chemical Engineering, Stanford University, are

nearing completion, and it is anticipated that the normal research activities can be resumed shortly.

APPENDIX 1

NASA Inf. Facil.

# ON THE DETECTION AND SIZE CLASSIFICATION OF NANOMETER SIZE METAL PARTICLES ON AMORPHOUS SUBSTRATES

by Klaus Heinemann

Eloret Institute, 1178 Maraschino, Sunnyvale, CA 94087

and Federico Soria

Consejo Superior de Investigaciones Cientificas

Instituto de Fisica Materiales

Serrano 117, 28006 Madrid, Spain

ABSTRACT

The detection and size analysis of small metal aggregates supported on amorphous substrates becomes increasingly difficult when the particle size approaches that of the phase contrast background structures of the support. Standard high resolution conventional transmission electron microscopy (CTEM) with subsequent analogue image analysis becomes inconclusive or fails for particles less than 1 nm in diameter, and clear differentiation of the particles from the background can only be made with considerable effort, typically involving several micrographs taken from the same specimen area under different imaging conditions. The TEM image contrast transfer mechanism is reviewed with emphasis on practical conclusions in this regard. In the 1-2 nm particle size range, particles can be distinguished from the amorphous background only when focus,

astigmatism, and specimen drift are optimally controlled. A deviation of only a few hundred nm from the optimum focus condition was, for example, found to increase the "apparent" diameter of 1.3 nm particles by as much as 0.4 nm. Furthermore, the electron exposure required to perform such microscopy may severely complexify the situation by radiation induced changes in specimen and support. These changes may be intensified by specimen contaminants and improperly controlled environment. An approach of digital image analysis, involving Fourier transformation of the original image, filtering, and image reconstruction is discussed with respect to the likelihood of unumbiguously detecting particles of less than 1 nm diameter on amorphous substrates from a single electron micrograph. Examples are given for the case of palladium deposits on carbon, alumina, and titania.

## INTRODUCTION

As is well known from the theoretical work of Scherzer [1] and the experimental work of Thon [2], the high resolution bright field image of an amorphous specimen such as a carbon or alumina support film contains, even if the film is perfectly planar and featureless, a multitude of contrast features that depend in amplitude, size, and distribution on the focus condition and on other imaging parameters such as illumination aperture (a decreasing aperture increases this contrast), acceleration voltage (decreasing voltage increases amplitude and size of contrast features), and astigmatism (affects directionality of the features).

For the purpose of this report, it is helpful to briefly review this well known phase contrast phenomenon with particular emphasis on the practical implications for high resolution microscopy of small particles. The dependence of reciprocal space frequencies (specimen details) imaged with optimum phase contrast on the deviation from the exact (Gaussian) focus $\Delta z$ is given by [3,4]:

$$\Delta z = 0.5 \left( C_s \alpha_o^2 - (2n-1)\lambda/\alpha_o^2 \right) \qquad (1)$$

In equ.(1) $C_s$ is the spherical aberration coefficient of the microscope objective lens, $\lambda$ is the electron wave length, $\alpha_o$ is the aperture angle corresponding to the imaged space frequency, and n is an integer with practical relevance in the range $-20 < n < 5$. Fig.1 shows a typical plot of $\alpha_o$ vs. $\Delta z$. It should be noted that, in accordance with a generally adopted convention, the underfocus region

has the positive sign (because it affects an increase of the focal length). Practical imaging conditions falling in the vicinity of one of the curves are necessary for resolution of that space frequency. The phase contrast amplitude reverses its sign between solid and dash curves. In practical interpretation of Fig.1, an image of a "Fourier-white" specimen, such as an amorphous specimen support film, will not be Fourier-white but contain spectral regions of space frequencies with alternating phase contrast amplitude, such as shown with the four diffractograms placed at their approximate respective $\Delta z$ positions at the top of Fig.1. The rings in the diffractograms are thus due to light optical diffraction at granular phase contrast structures that appear in the real image and have certain size and distance relationships with each other but no conclusive practical relation to the specimen itself. The structures may appear so strong in contrast that it would seem impossible to distinguish images of real particles from them if these particles are in the same general size range. (These background structures are, of course, the reason why the tendency for small particle work has been to use single crystal support films [5-9]).

An example of the focus dependence of the phase contrast structures is shown in Fig.2 for the case of a plain carbon film with three marker particles (circled) demonstrating that the same specimen area is shown in each micrograph. From (a) to (d) the focus was changed from $\approx$50 nm to about 500 nm. The diffractograms were taken from the same area. It is obvious that any sub-nanometer size particles would be entirely lost in this multitude of substrate related contrast features.

On the basis of the size of these phase contrast background structures, we divide the task at hand in two groups, (i) particles less than about 1 nm in size, where the particle and background structure sizes are about the same and, consequently, very difficult to separate, and (ii) particles larger than about 1 nm where the particles generally stand out from the background. The latter category allows the use of conventional particle size analyzers, the former requires more elaborate approaches for detection and size analysis of deposit metal particles.

## GENERAL IMAGING REQUIREMENTS

It is helpful to consider some practical implications of the phase contrast transfer characteristic of a TEM objective lens such as shown in Fig. 1 for the case of 100 kV acceleration voltage and $C_s$ = 2.25 mm. In practice, the illumination aperture $\alpha_{1/1}$, the chromatic aberration

$\delta_{z_F}=C_F(\Delta U/U + 2\Delta B/B)$ (U is the acceleration voltage, B is the magnetic field of the objective lens [3]), the specimen support film thickness t, and the prevailing astigmatism $\Delta a$ have finite values that cause the imaging conditions applicable to Fig.1 to take the shape of an error ellipse rather than a mathematical point [4]. In this representation, $\alpha_{1/1}$ would determine the vertical axis, and a combination of t, $\delta_{z_F}$, and $\Delta a$ the horizontal axis of this error disk. If it includes the vicinities of more than one curve in Fig.1, this

would lead to an effective reduction or even extinction of the resulting phase contrast transfer (resolution). We have included such an error ellipse for an illumination aperture angle of approximately $1.5 \times 10^{-3}$ radians and a specimen thickness of 50 nm (and assuming perfectly corrected astigmatism and negligible residual chromatic aberration) in three defocus positions. Specimen details of 0.4 nm can well be resolved at 130 nm underfocus; in the exact focus conditions ($\Delta z=0$; Gaussian focus) or at a larger defocus (500 nm in the example), neighboring contrast curves of opposite sign are included in the error area, and 0.4 nm phase contrast resolution will be strongly impeded.

This circumstance can be utilized as a benefit for the task of imaging small particles. Due to the higher atomic scattering amplitude of the metal atoms when compared to the atoms usually comprising the support material, amplitude contrast can be used as most useful contrast mechanism. This can be done by a combination of two microscopy conditions: (i) by increasing the illumination aperture angle such that for a wide space frequency band a significant reduction of the phase contrast occurs (at the chosen focus setting), and (ii) by choosing a defocus setting most prone to yield the least phase contrast selectivity. These conditions are met in the "phase contrast minimum" region (typically some 50 nm below the Gaussian focus) and with an illumination aperture large compared to the separation of the two critical phase contrast transfer curves (with n=1 and n=2) in that $\Delta z$ region. In practice, $\alpha_{1,11}$ should be $> 2 \times 10^{-3}$ radians. It would of course not pay to to try to wash out unwanted phase contrast structures by deliberately using a thick

specimen support film. In fact, the support film must be as thin as possible if the weak amplitude signal of very small metal particles is to be distinguished from the (weak yet not negligible) thickness-dependent amplitude signal of the substrate.

Other techniques that one might consider for imaging very small supported metal particles by CTEM concentrate on the elimination of the phase contrast selectivity phenomenon altogether. This can be achieved by using strongly incoherent illumination, such as with an annular condenser aperture [10], or by combining substantially coherent illumination with interference of diffracted beams only, such as in central dark field microscopy [3] or selected-zone dark field microscopy (SZDF; [11]). The disturbing space frequency contrast transfer selectivity can also be decreased by using interference between the undiffracted beam and only one of the diffracted beams (such as with a semi-circular aperture [12] or with a combination of annular condenser and annular objective apertures [3,4,10,11]). Phase shift objective aperture diaphragms [13] have also been attempted to reduce the contrast transfer selectivity. Whereas SZDF microscopy is powerful indeed for imaging and mapping ordered structures [3,11,14], it fails for particles smaller than about 1.5 nm in size, in particular if the atoms comprising the particles are not (yet) well ordered. Recent research on small particles in our laboratory [15] has shown that the structure of very small metal clusters may indeed not be well developed. For imaging nanometer-size particles, it is, therefore, advisable to select a technique that does not depend on Bragg diffraction as contrast mechanism and, thus, does not a-priori exclude poorly structured

particles. Microscopy with other unconventional objective apertures, such as semi-circular apertures allowing the undiffracted beam to barely pass in the center of the semi-circle [12] or phase plates [13] have seldom been used. It have been mostly experimental difficulties, such as excessive astigmatism caused by charging of the aperture due to an uncontrolled build-up of contamination at the aperture, and of course manufacturing difficulties of the aperture itself that have prevented these techniques to become practical alternatives for imaging sub-nanometer size particles.

## PARTICLE IDENTIFICATION BY CORRELATION

The circumstance that the transfer of phase contrast of sub-nanometer specimen distances can be manipulated with the focus setting and other imaging parameters suggests that one criterion of definite recognition of very small metal particles on amorphous substrates might be the spatial correlation of imaged intensities in several micrographs taken under different microscopy conditions that affect the amplitude contrast of the particles only little but cause substantial differences in phase contrast image features. In practice, any one feature that consistently appears in all of these micrographs is likely to be a particle, whereas features visible only in a minority of the micrographs are identified as merely support related. Unless an elaborate computerized image comparison system is available, this method is prone to be tedious and time-consuming. An example (Pd/carbon) is given in Fig.3. Lines (a) and (b) were taken

with a small objective aperture near the Gaussian focus and in slight underfocus, respectively. Line (c) was was taken near the Gaussian with a large objective aperture. Line (d) is a superposition of four exposures at 100 nm focus difference (starting at Gaussian focus and going toward underfocus) using the same large aperture as in (c). Whereby it would be highly questionable to identify palladium particles in any one individual micrograph, the correlation in all four images (row (c)) suggests with fair accuracy that those intensities that coincide in all four images are particles. The correlated particles are highlighted in row (c). Row (a) shows the respective optical diffraction patterns. In this particular example of Pd/C, the correlation method established that the saturation particle number density had already been reached in this very early stage of growth (see [15]).

## PARTICLE RECOGNITION AND SIZE ANALYSIS WITH IMAGE ANALYZERS

Once the particles are large enough to be easily detected on an amorphous substrate, use of an analogue or digital image analyzer is effective for the next steps of a deposit/substrate/environment analysis, such as counting, area coverage measurements, and particle size distribution determination.

Typically, the instruments with which such analysis is performed consist of a video system and an image processing system. For an analysis of palladium particles on alumina, titania, and carbon

substrates, we have employed a Quantimet 720 facility with epidiascope-TV pickup of EM images printed at 1,000,000 X magnification. A 30-mm focal length TV camera objective lens was used, giving a resolution of 0.09 nm per pixel. A major difficulty is shading correction of the background which is usually somewhat uneven over the size of the image to be analyzed. The built-in shading corrector is designed to correct for uneven epidiascope illumination only. Its use in conjunction with an EM micrograph with small particles is only advantageous after strong defocussing the image with the TV camera objective lens, blurring the individual particles to sizes larger than the individual shading correction elements which are typically 10x10 to 15x15 pixels. Employing shading correction to focused images can actually have a distinct negative effect in that this tends to lower the contrast of the particles with respect to the background. On the other hand, particle size analysis may become meaningless or inconclusive without proper shading correction that assures that the particle contrast discrimination occurs always at the same level with respect to the substrate.

In order to avoid systematic errors stemming from the subjective choice of the image discrimination levels, we chose a method whereby each shading corrected image was analyzed with a series of discrimination settings, starting well below and ending well above what would seem the most appropriate setting. Definite conclusions were drawn only with respect to those features in the resulting histograms that were reproduced in each or most of the individual measurements. In addition, several micrographs of the same specimen type were evaluated.

An example of a specimen with approximately 2 nm diameter particles of palladium on an amorphous (30 nm thick) $TiO_2$ film is shown in Fig.4. The corresponding size distribution histograms are shown for four discrimination settings. Common to most of the individual histograms are (a) a rapid decrease of the particle count for very small size classes, (b) a minimum at about 1.1 - 1.3 nm, (c) a major peak at about 2.1 nm particle size, and (d) three minor peaks (at 1.4, 2.4, and 3.0 nm. We attribute the initial portion of the histograms to phase contrast background features and only identify those histogram size classes beyond 0.8 nm as palladium particles. Fig.5 shows the corresponding results for a sample that, under otherwise identical conditions, had been subjected to a shorter deposition time (about 1/3 of that used for Fig.4). The main peak of the size distribution is now at 1.3 nm, and a minor peak is at 1.8 nm. Fig.6 shows the same specimen detail area and corresponding histograms, with the only difference being the focus setting in the original micrograph (about 200 nm vs. 100 nm underfocus, respectively). This relatively minor focus shift resulted in an apparent increase of the mean particle size by approximately 0.4 nm to 1.7 nm, and a shift of the minor peak to about 2.3 nm. A second minor peak now appears at 0.8 nm particle size, but we question that this is clearly a particle peak and not merely a remnant from the substrate phase contrast features.

## OPTICAL IMAGE FILTERING

It has been suggested to attempt to eliminate the phase contrast predominance in an amorphous substrate with respect to nanometer size metal particles by filtering out certain space frequencies in the diffractogram [16] and subsequent image reconstruction. This can be accomplished on-line with optical methods (starting from the original micro-negative) or with a computer.

An example of the on-line optical approach is presented with Fig.7, showing a Pd/C deposit with 1.5 nm mean particle size near Gaussian focus (top) and at approximately 200 nm underfocus (bottom line). In (a), the optical diffraction patterns (diffractograms) of the specimen area shown in (b) are shown. They contain, next to the usual substrate-related intensity pattern, a brighter zone in the center (see marker) which stems from diffraction at the particles and indicates, by calibration of the diffractogram, their approximate size distribution. If a small aperture is inserted in the diffractometer set-up, filtering out all space frequencies substantially larger than this particle-related central region, and if subsequent optical image reconstruction is made, the micrographs of Fig.7(d) result. They exhibit, in addition to inherent contrast reversal, a significantly increased contrast between the particles (bright) and the background. Furthermore, the difference between the two focus settings, affecting the particle contours in the original micro-negatives, no longer exists. Fig.7(c) shows for reasons of completion the same reconstructed images without optical space frequency filtering. As expected, identification of the particles is

here somewhat more difficult on the more uneven background when compared to the filtered images (d).

## COMPUTERIZED IMAGE FILTERING

Optical filtering is in practice limited to a few extreme conditions, such as high-pass filtering (i.e., filtering large specimen distances), using a beam stop aperture, low-pass filtering, using a circular aperture (Fig.7), or a combination of both, using an annular aperture. Furthermore, it seems difficult to eliminate secondary diffraction effects at this aperture and from other components of the optical bench in the reconstructed image (see circular features in Fig. 7(d)).

Image filtering could become more meaningful and powerful if, instead of rigorous low/high pass filtering, that and only that part of the Fourier spectrum (diffractogram) could be eliminated that corresponds to the support background, while the entire Fourier spectrum of the particles would remain. For this, or in practice for any filtering other than direct low/high pass filtering, digital image processing would seem the appropriate means. The following tasks would be involved: (a) digitizing of the primary image (256 x 256 pixels and 128 grey levels are generally sufficient and warrant reasonably short computing times even with state-of-the-art microcomputers; (b) Fourier transformation of this image (the Fourier coefficients must be separated in real and imaginary parts for further manipulation);

(c) 2-dimensional video presentation of the Fourier spectrum (diffractogram) for easy recognition of main characteristics such as residual astigmatism and focus setting; (d) mathematical manipulation of the Fourier coefficients (such as multiplication with a function of the space frequency); (e) reconstruction and video presentation of the manipulated image; and, of course, (f) counting, area coverage, and size analysis measurements with the reconstructed image.

## DISCUSSION AND PROSPECTS

### Basic Differences Between "Standard" High Resolution TEM and Small Particle Imaging

Probably the single most important conclusion from this work is that the requirements for (high-resolution) detection and imaging of very small deposit metal particles on amorphous substrates are substantially different from the "standard" high resolution CTEM imaging requirements. For example, lattice planes are easiest resolved at a defocus setting near the apex of a phase contrast curve (Fig.1) suited for the space frequency to be resolved [3]. For example, under axial illumination conditions at 100 kV acceleration voltage, palladium {111} lattice planes (0.225 nm spacing) would best be resolved at about 615 nm underfocus (with the n=22 chracteristic, using the relation $\delta_z(\alpha_o)=C_s\,\alpha_o^{n}$ [3]), if the spherical aberration coefficient happens to be 2.25 mm. Images of 0.45 nm spacings of mica lattice planes would require an optimum defocus of 150 nm and would use the apex of the n=-1 curve. This indicates that the optimum defocus may be substantially below the Gaussian focus setting, whereas for small particle detection and imaging the region near the Gaussian focus (some 50 nm underfocus) is clearly preferable. Furthermore, relatively large illumination angles $\alpha_{illum}$ are generally preferable for small particle resolution on amorphous substrates, whereas small illumination apertures are often used for standard high resolution microscopy, because this allows easier astigmatism correction (better recognition of the phase contrast background

structures used for this purpose) and generally favors imaging of phase contrast features (which are far too often indiscriminately considered desirable and interpreted as intrinsic specimen details). Lower acceleration voltages (50 - 100 kV) are also more effective for small particle imaging, because this helps emphasize the critical amplitude contrast required for this task, as opposed to voltages up to 1000 kV that are often considered desirable for ultimate resolution microscopy. As example, we point to Fig.8, which shows the same sample area of Au/C for the case of 25, 50, 75, and 100 keV beam energy, clearly indicating the tendency of decreasing contrast with increasing beam energy (see also [17]).

Another important difference is that it is often essential to work with beam intensities at which particle/substrate interaction is minimized. As was shown in ref. [18], this interaction may be substantial and may require operating the TEM at minimum required magnification and/or with high-speed image recording [19]. Typically, an electron optical magnification of 100,000 X may well be all that is required to image sub-nm size particles. Using standard TEM photographic material with a resolution capability of better than 15 micrometers, details of 0.15nm can then be resolved (but require proper light-optical magnification of the micronegatives). Current densities of the order of $< 10^{-1}$ A/cm$^2$ are sufficient for such microscopy, as opposed to intensities over 10 A/cm$^2$ that are often used with state-of-the-art microscopes operating at 500,000 to 1 Million X electron optical magnification, and further reduction of the intensity to the $10^{-3}$ A/cm$^2$ range is possible with efficient image intensifiers, while maintaining sub-nm resolution [19].

Techniques Required for Small Particle Imaging by CTEM

Probably the most persuasive argument for operating near the Gaussian focus is presented with Figs.5 and 6 which clearly show that the apparent particle size is decisively affected by the focus setting, all other parameters being equal. Whereas this observation alone does not assure that particle size measurement for conditions nearest to the Gaussian focus are most representative of the specimen, there are other well-known persuasive reasons that do favor this interpretation. In particular, the contrast transfer is steepest at this focus condition (but does not include Fresnel sholders that tend to artificially enhance the contrast of the underfocused or overfocused image), which is critical for correct discrimination with image analyzers. Our findings show that a deviation of as little as 100 nm in defocus can shift the measured size classes by as much as 0.4 nm. Generally, particles appear larger when imaged out of focus.

The phase contrast transfer characteristic (Fig.1) is a practical tool to taylor optimum imaging conditions for the task at hand. In particular, it suggests the most appropriate illumination aperture angle and focus settings to use.

Image analyzers can be most helpful only for particles > 1nm in diameter, and only when used in the particle size analysis mode, because it is only then that discriminated support background features can be distinguished from real particles (see the first

steep negative slope in the histograms of Figs.4-6). Particle counts should be made from particle size distribution histograms, whereby the initial counts that are most likely due to substrate features must be discounted. For the same reason, area coverage measurements must be interpreted with care. However, the error stemming from indiscriminately including very small background features in this measurement is not as significant in this case, because even many small background features may overall contribute only relatively little to the total area count which is, of course, dominated by the larger particles.

Shading correction is vitally important for obtaining meaningful size distributions. Without shading correction, particles would be discriminated at various threshhold levels within one statistical sample. Since the contrast slope is finite (yet relatively steepest if the micrograph was taken at Gaussian focus, as mentioned earlier), the measured size of a particle depends on where within this slope the discrimination took place. The results of histrograms would be unduly averaged, eliminating the possibility of revealing characteristic size classes, if the discrimination levels were not equalized throughout the entire analyzed micrograph area by shading correction. On the other hand, observing the same size classes in well shading-corrected images using <u>different</u> discrimination settings is a most positive evidence that the observed size classes are real.

For particles less than 1 nm in mean size, image analyzers are of little help, and the correlation method seems essential for positive particle identification. It may, however, be sufficient to correlate

intensity features in two or three micrographs taken with different focus settings, whereby the phase contrast transfer characteristic (Fig.1) may be helpful to select the most appropriate different focus settings. Of course, a size distribution cannot be made in this case.

Optical diffractograms are most helpful for establishing the mean size of a particulate deposit. This can be done by measuring the intensity ring in the center of the diffractograms stemming from diffraction at the particles (Fig.7). On-line optical filtering (Fig.7d) increases the contrast of the particle to such a degree that counting with image analyzers becomes more feasible and accurate, while unwanted background features are eliminated from the count. However, the inherent loss of sharpness of the particle contours would render subsequent size analyses with an image analyzer meaningless. It remains to be seen if computerized image filtering will be able to enhance foth the detectability and the size analysis of small nanometer-size particles.

Size Classes for $Pd/TiO_e$

The results for palladium deposited on titania indicate that particles in two major size classes were formed 1.3 nm and 1.8 nm for the thinner deposits, and 1.4 nm and 2.1 nm for those samples subjected to a longer deposition time. It is tempting to correlate the individual, measured peaks in the size distribution histograms with discrete particle sizes that would be expected if the particles consisted of close-packed spheres with "shells." In a recent

communication [20], palladium particle sizes of 0.8nm, 1.4nm, 1.7nm, and 2.6nm were discussed as corresponding to 13, 55, 135, and 490 atoms, respectively. Sattler [21] found 13, 55, and 147 atoms to be "magic" numbers in clusters. The particles in our present sample may have been subjected to changes due to exposure to air and/or to hydrocarbon contaminants and reactions during the microscopy, which is known to influence the particle size [22,23]. There is nevertheless quite reasonable agreement between the size classes observed in this study for $Pd/TiO_2$ and the "magic numbers" 55 and 147 which point to icosahedral or cubo-octahedral particle structures. Further analysis work, especially done in-situ under controlled environment conditions [21-24], is highly desirable to draw more definite conclusions in this regard.

ACKNOWLEGEMENTS

Part of this work was performed at the NASA Ames Research Center in Moffett Field, California, under NASA-Grant No. NCC2-283 to Eloret Institute. The image analysis work was performed at the Instituto de Fisica Materiales, CSIC, Madrid, under program No. CCB 84/09/009 sponsored by the U.S.-Spain Joint Committee for Scientific and Technological Cooperation. We also greatfully acknowledge financial support by ALCOA Foundation and interesting discussions and preliminary feasibility studies for computerized image filtering and reconstruction with Dr. Julian Bescos of the Instituto de Optica, Serrano 121, CSIC, Madrid.

REFERENCES


[1] O. Scherzer, J. Appl. Phys. 20, 20, 1949.

[2] F. Thon, Z. Naturforschung 207, 1, 1965.

[3] K. Heinemann, Optik 34, 113, 1971.

[4] H. Poppa, in "Epitaxial Growth," Part A, Academic Press, New York, 1975, p.215.

[5] H. Poppa and K. Heinemann, Optik 56, 183, 1980.

[6] T. Komoda, I. Nishida, and K. Kimoto, J. Electron Microscopy 19, 105. 1970.

[7] H. Hashimoto, A. Kumao, H. Yotsumoto, and A. Ono, Jap. J. Appl. Phys. 10, 1115, 1971.

[8] K. Mihama and N. Tanaka, J. Electron Microscopy 25, 65, 1976.

[9] S. Ijima, Proceed. 34th EMSA, G.W. Bailey, Baton Rouge, Claitor's Publ. Div., 1976, p.568.

[10] K. Heinemann and H. Poppa, Appl. Phys. Lett. 16, 515, 1970.

[11] K. Heinemann and H. Poppa, Appl. Phys. Lett. 20, 122, 1972.

[12] F. Thon, Proceed. Europ. Congr. EM, Rome, 1968, V.1, p.127.

[13] F. Thon and D. Willasch, Proceed. 29th EMSA, G.W. Bailey, Baton Rouge, Claitor's Publ. Div., 1971, p.38.

[14] K. Heinemann, M.J. Yacaman, C.Y. Yang, and H. Poppa, J. Crystal Growth 47, 177, 1979.

[15] H. Poppa, R.D. Moorhead, and K. Heinemann, Thin Solid Films 128, 251, 1985.

[16] F. Thon and B.M. Siegel, B. Bunsenges. Phys. Chem. 74, 1116, 1970.

[17] K. Heinemann and G. Moellenstedt, Optik 26, 11, 1967

[18] K. Heinemann and H. Poppa, Ultramicroscopy, in print.

[19] K. Heinemann and H. Poppa, Proceed. 31th EMSA, G.W. Bailey, Baton Rouge, Claitor's Publ. Div., 1973, p. 610 and 612.

[20] P. Gallezot, M. Avalos-Borja, H. Poppa, and K. Heinemann, Langmuir 1, 342, 1985.

[21] K. Sattler, in "Current Topics in Mat. Science," ed. E. Kaldis, Elsevier Publ., B.V., 1985, p.1.

[22] K. Heinemann, T. Osaka, H. Poppa, and M. Avalos-Borja, J. Catalysis 83, 61, 1983.

[23] K. Heinemann, T. Osaka, and H. Poppa, Ultramicroscopy 12, 9, 1983.

[24] K. Heinemann and H. Poppa, J. Vac. Sci. Technol., in print.

FIGURE CAPTIONS

Fig.1 Phase contrast transfer characteristic for $\lambda$(100 kV)=0.0037 nm electron wave length and $C_s$=2.25 mm spherical aberration coefficient. Diffractograms (top) correspond to carbon film images taken at the respective focus settings (-30nm, 140nm, 230nm, and 310nm).

Fig.2 Plain carbon film with three marker particles taken at increasing underfocus.

Fig.3 Identification of Pd particles on carbon by contrast feature correlation in four micrographs (same specimen area) taken under different imaging conditions. Left: corresponding diffractograms; right: identified Pd particles are highlighted.

Fig.4 Particle size analysis of Pd/$TiO_2$ deposit, obtained with four different grey level discrimination settings (dash, solid, dash-dotted, and dotted curves).

Fig.5 Particle size analysis of thin Pd/$TiO_2$ deposit (half deposit thickness of specimen analyzed in Fig.4).

Fig.6 Same as Fig.5, but with 100 nm increased underfocus used in electron micrograph.

Fig.7 Pd/C taken near Gaussian focus (top) and at about 200 nm underfocus (bottom); the reconstructed images were taken before (c) and after (d) optical filtering of essentially all reciprocal space

frequencies beyond the intensity stemming from the particles (shown in diffractogram (a)).

Fig.8 Au/C taken with Hitachi H500H CTEM at 25, 50, 75, and 100 kV acceleration voltage under otherwise identical conditions.

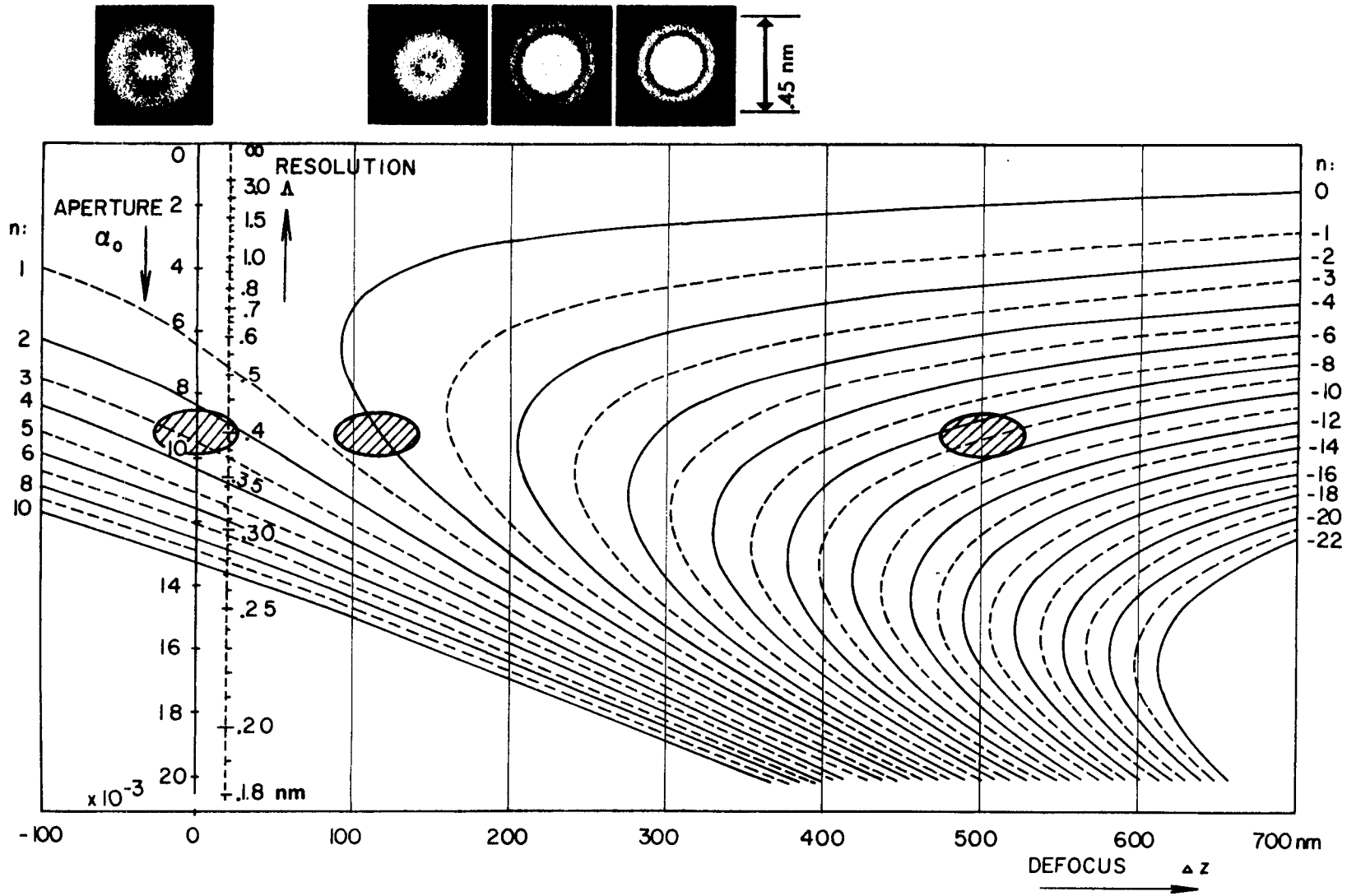


FIG. 1

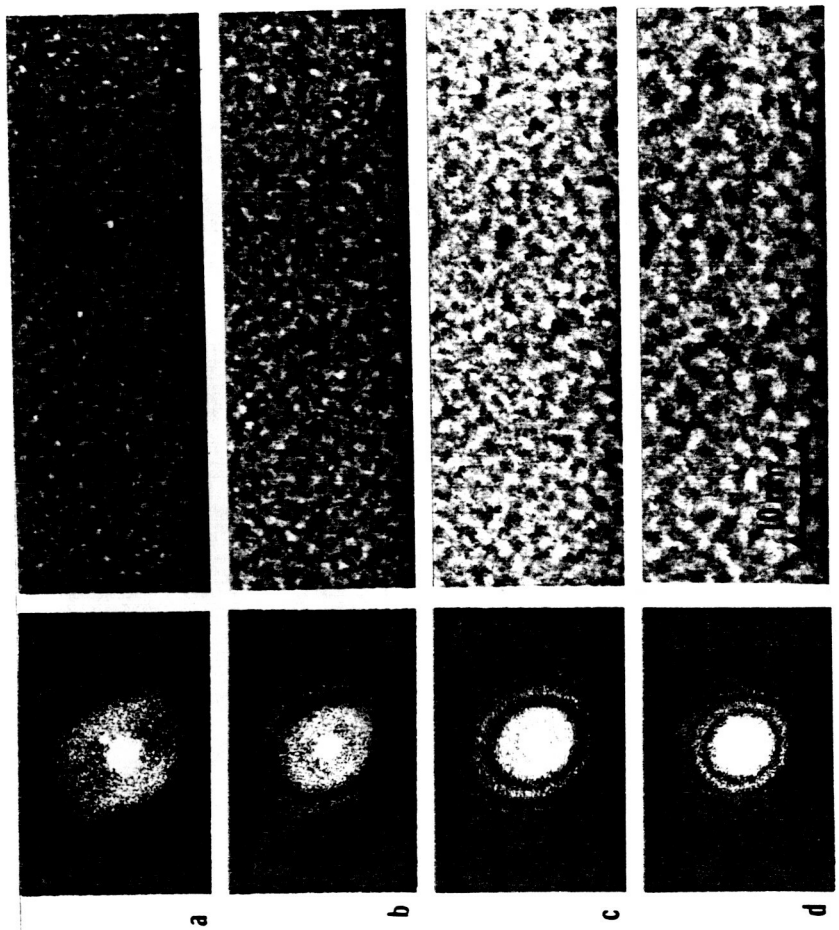


FIG. 2

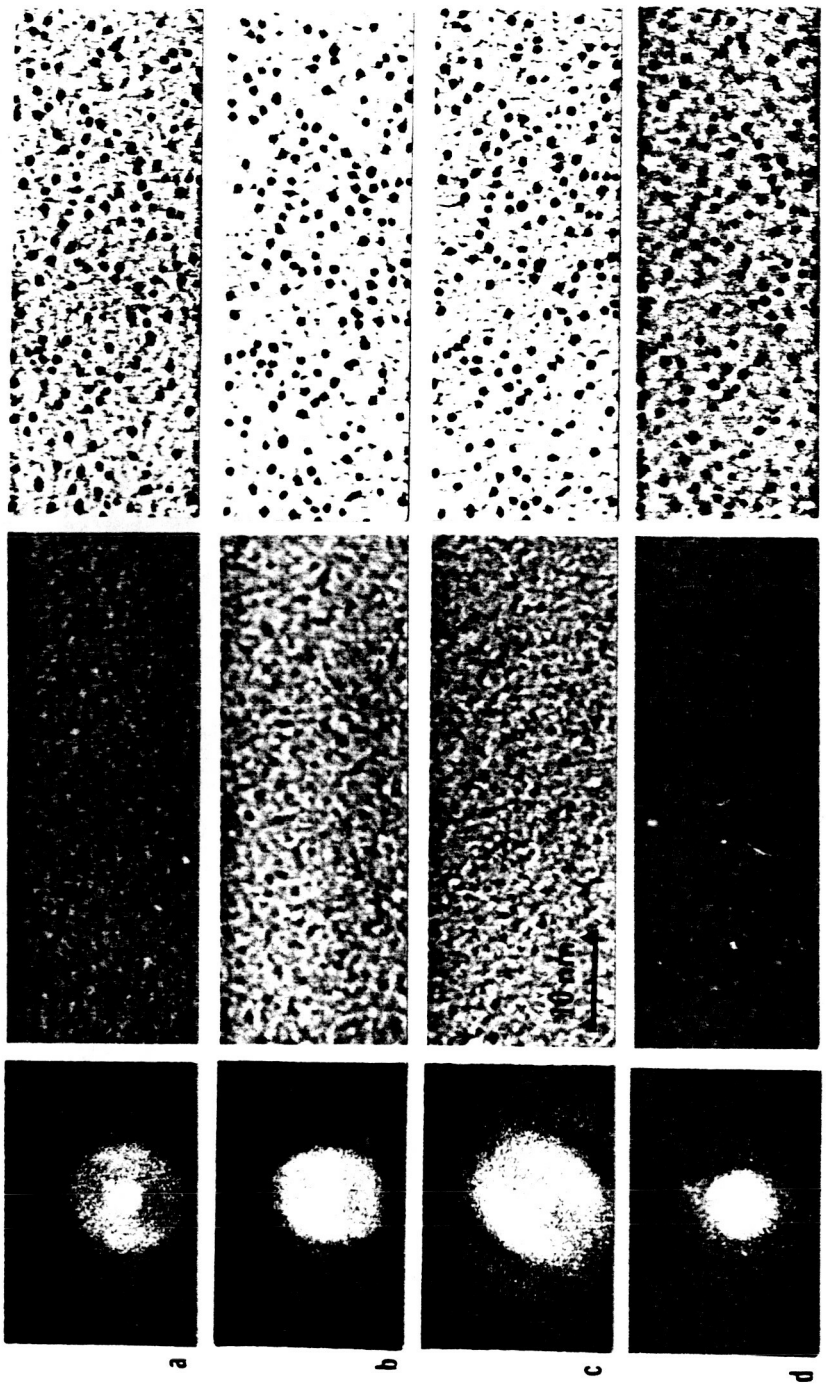


FIG. 3

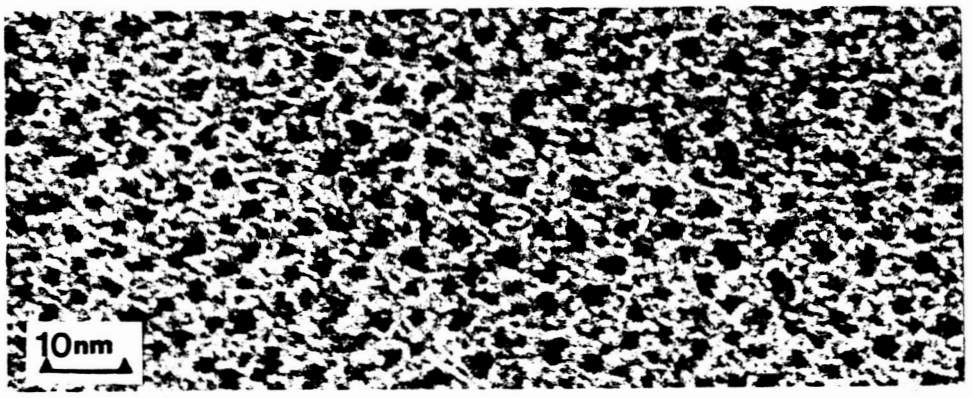


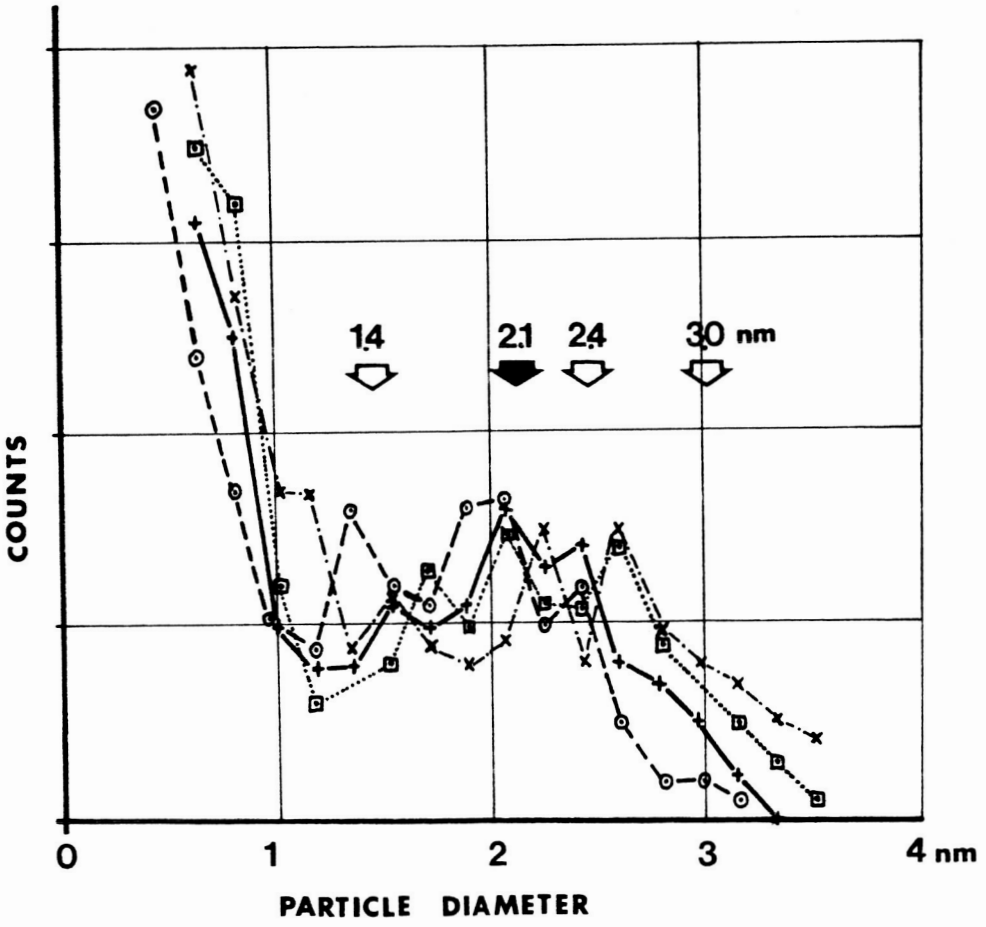


FIG. 4

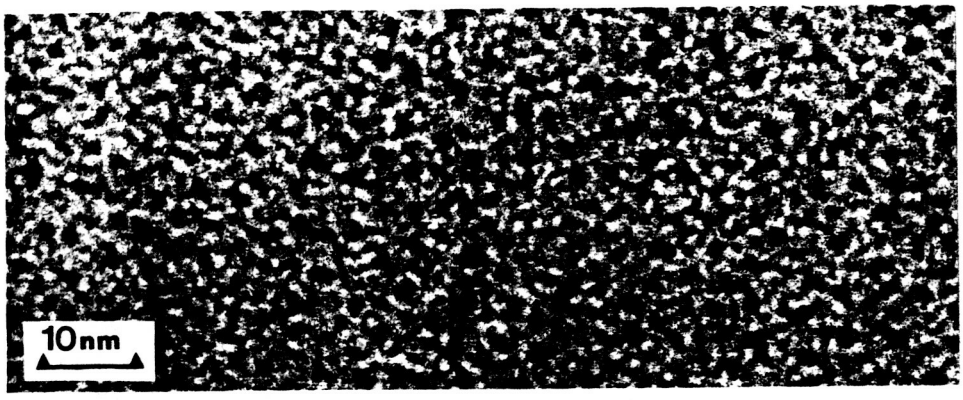


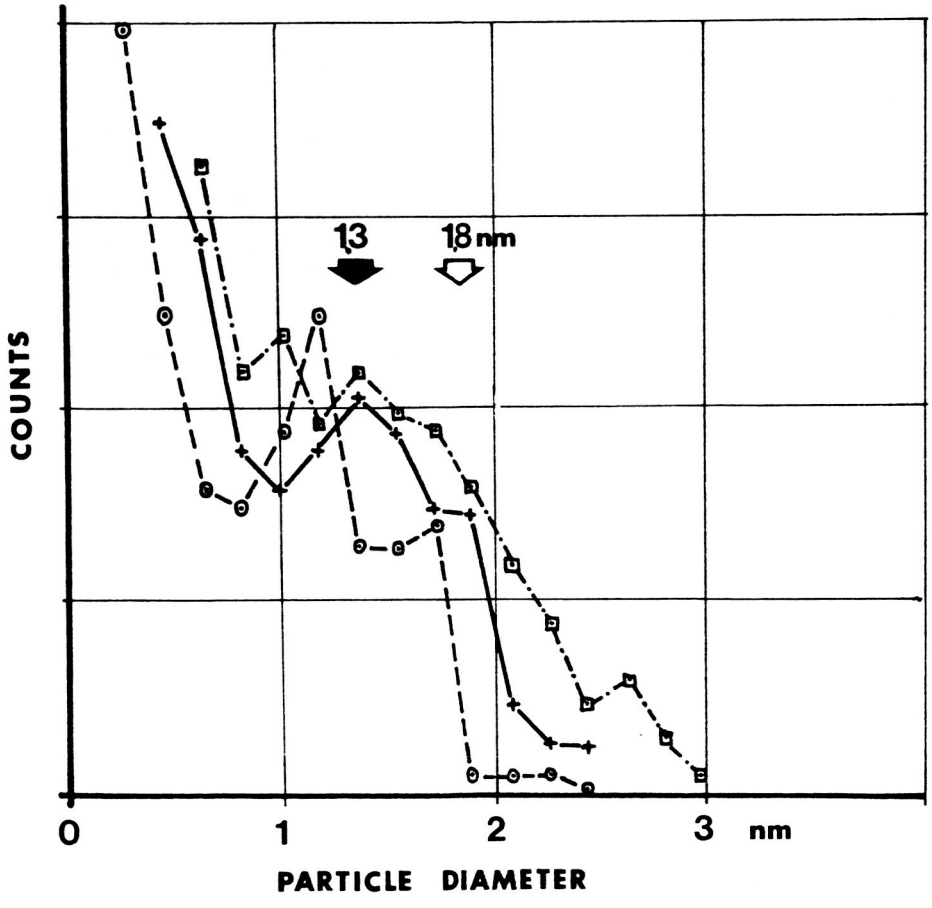


FIG. 5

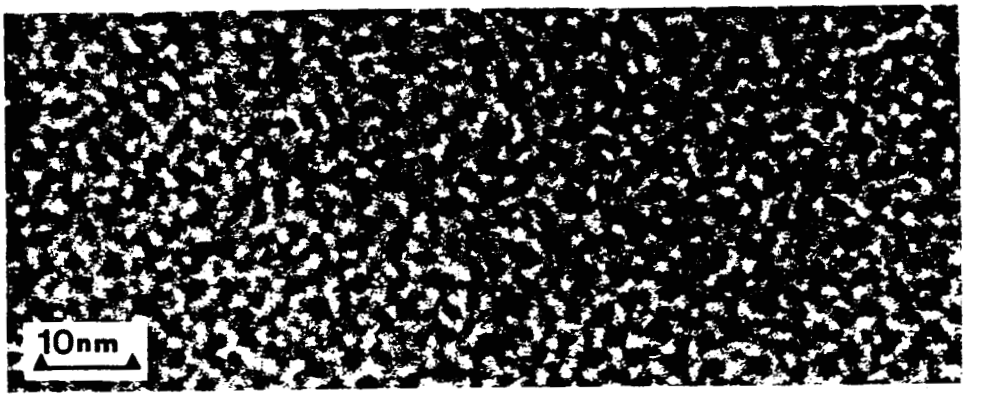


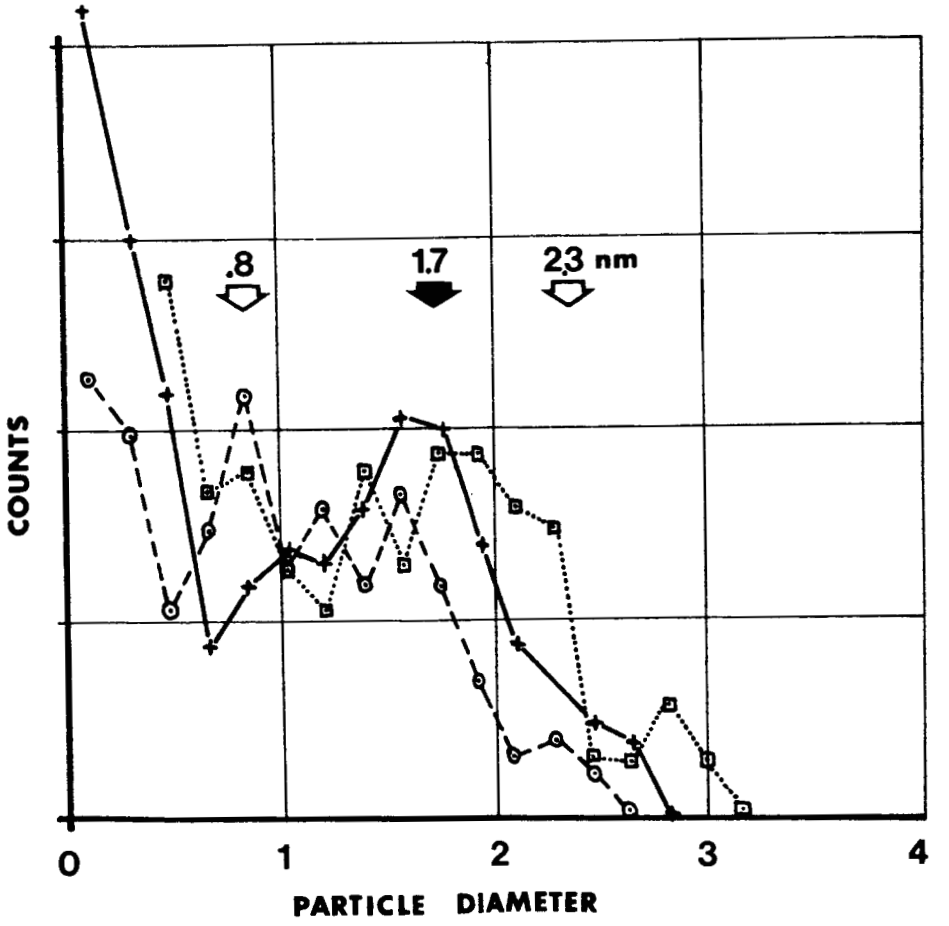


FIG. 6

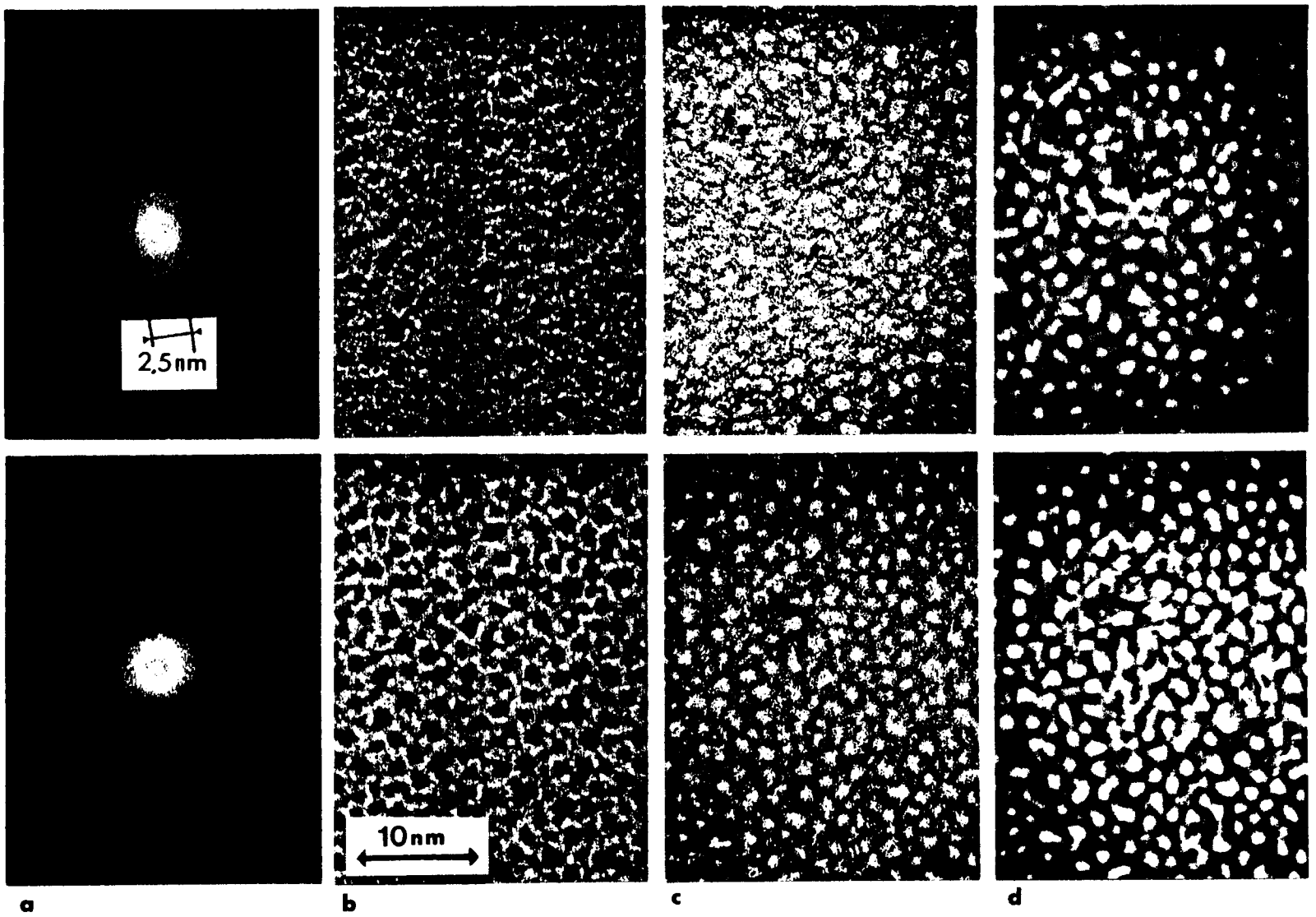


FIG. 7

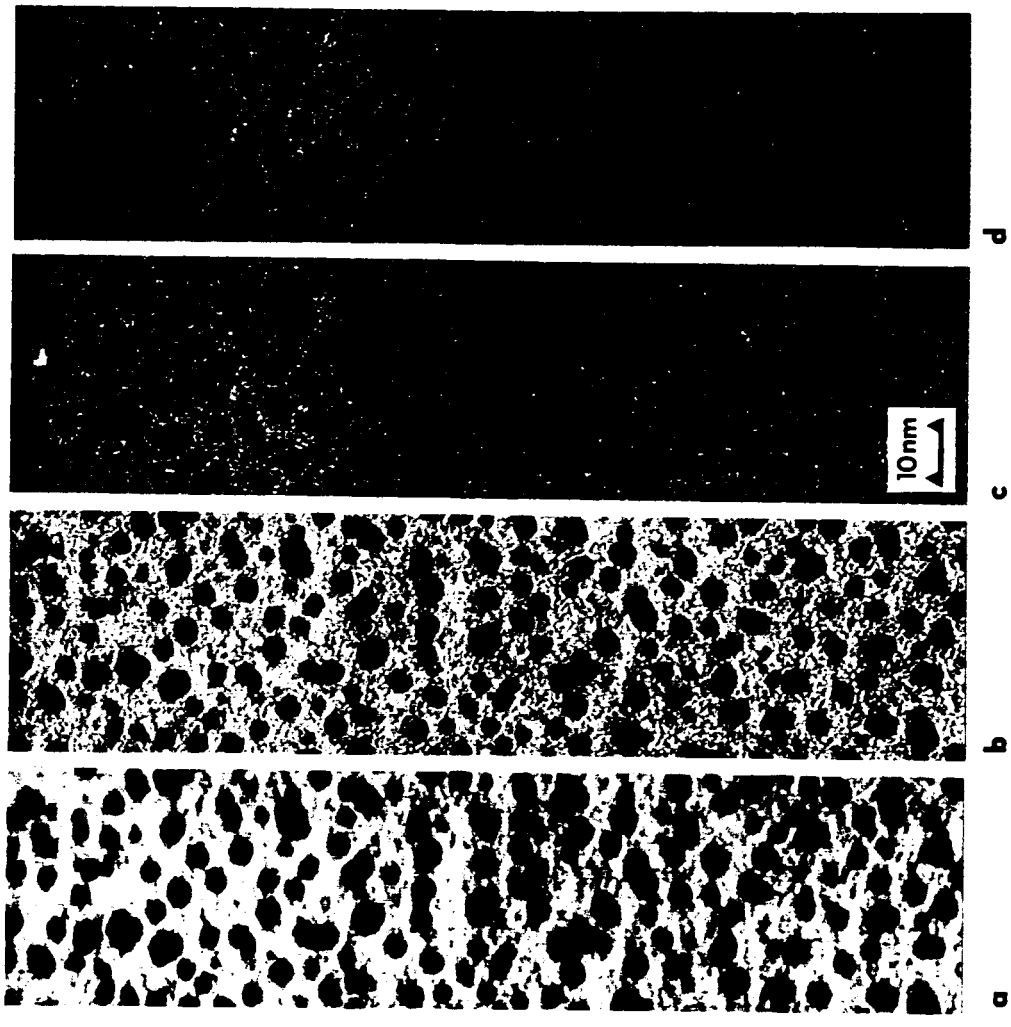


FIG. 8